https://doi.org/10.1007/s41230-019-9067-9

Microstructure and mechanical properties of AZ91 magnesium alloy with minor additions of Sm, Si and Ca elements

Redeemina Comfort Bonnah, Yu Fu, *Hai Hao

Key Laboratory of Solidification Control and Digital Preparation Technology, School of Materials Science and Engineering, Dalian University of Technology, Dalian116024, Liaoning, China

Abstract: The effects of Sm, Si and Ca on the microstructure and mechanical property of AZ91 magnesium alloy were investigated by means of optical microscopy (OM), differential scanning calorimetry (DSC), scanning electronic microscopy (SEM), X-ray diffraction (XRD) and tensile testing. The results indicated that the addition of 1.5 wt.% Sm with or without 0.8 Si/Ca led to a decrease in the volume fraction of the β-$Mg_{17}Al_{12}$ phase and the formation of the intermetallic compounds of Al-Sm, Mg_2Si, MgAlCa and Al_2Ca. The microstructure of AZ91 alloy was significantly refined and distribution became discrete with additions of Sm and Ca; the average grain size of the α-Mg matrix was reduced from 239.7 ± 16.9 μm to 66.34 ± 5.10 μm. The AZ91-Sm-Ca alloy exhibited a good combination of yield strength at 135 MPa, ultimate tensile strength at 199 MPa and elongation at 4.32%, which was ascribed to grain refinement strengthening. Furthermore, the T6 treated AZ91-Sm-Ca alloy possessed yield strength of 154 MPa and elongation of 7.1%, which was due to grain refinement strengthening and reduction in discontinuous precipitates.

Key words: AZ91; Sm; Ca/Si; grain refinement; mechanical properties

CLC numbers: TG146.22 **Document code:** A **Article ID:** 1672-6421(2019)05-319-07

The introduction of luxuries components and extra safety measures in the automobile increased its weight, leading to a higher fuel consumption and subsequent release of greater amounts of greenhouse gases (e.g., CO_2). This effect motivates wide spread use of magnesium alloys [1-3] as they have many advantages including low density, high specific strength and stiffness, excellent machinability and good recyclability, which generates application value in many fields such as aerospace, automotive, and telecommunication industries. AZ91 magnesium alloy is the most widely used to fabricate commercial structural components due to the good blend of room-temperature strength and ductility [1-3]. However, its utilization is limited to the interior parts in the cast products, since the reticular β-$Mg_{17}Al_{12}$ phases presenting at grain boundaries and dendritic arms have a negative effect on mechanical properties [4]. Grain refinement plays an important role in enhancing mechanical properties of magnesium alloys, especially magnesium alloys with a close-packed hexagonal structure. Grain refinement can effectively reduce hot tearing tendency and shrinkage porosity, improving creep properties and corrosion resistance [5]. Alloying is one of the efficient methods to reduce grain size and modify the morphology of the second phase.

Some researchers reported that the addition of samarium (Sm) to magnesium alloys could refine the grain and enhance mechanical properties [6-10]. The Sm-containing AZ31, AZ61, AZ91 and AZ92 alloys formed a new Al_2Sm compound, resulting in a reduction in the area fraction of the β-$Mg_{17}Al_{12}$ phase. In addition, the Al_2Sm phase formed heterogeneous nuclei for the Mg grains, improving elevated temperature resistance as well as the corrosion resistance of Mg-Al alloys [11-15]. Chen et al. [8] found that the combined additions of Ca and Sm significantly refined the microstructure in the AZ61 alloy and the mechanical properties were improved due to the formation of Al_2Sm and Al_4Sm phases, but grain refinement was not realized. Addition of silicon (Si) to magnesium generates thermally stable intermetallics of FCC structure Mg_2Si phase [16]. The Mg-Al-Si

***Hai Hao**

Male, born in 1969, Ph.D., Professor. His research interests mainly focus on solidification control, casting technology of light metals and porous materials. He has published more than one hundred scientific and technical papers. E-mail: haohai@dlut.edu.cn

Received: 2019-05-21; Accepted: 2019-07-26

alloy has been considered as a potential elevated temperature resistance magnesium alloy. For example, Si has been used to improve the microstructure, fluidity, mechanical properties and precipitation behavior of the Mg-6Al alloy [17-18]. Adding Ca to Mg alloys can increase the ignition temperature of Mg alloys, and result in the significant grain refinement and formation of intermetallic compounds at grain boundaries, which improves the thermal stability of the β-phase and the room and high temperature strength [19-21].

The aim of this work is to study the influence of Sm on the microstructure, grain refinement and mechanical properties of AZ91 alloys. Besides, the combined addition effects of Sm and Si or Ca are further investigated in terms of microstructure and mechanical properties.

1 Experimental procedures

AZ91 alloy was prepared by commercial pure Mg (≥99.95%), Al (≥99.7%), Zn (≥99.99%) ingots and a master alloy of Mg-3.5Mn. Alloying elements, Sm, Si and Ca were added to the AZ91 alloy in the form of Mg-30Sm, Mg-10Si and Mg-20Ca master alloys, respectively. The compositions of the studied alloys are shown in Table 1, obtained by the X-ray fluorescence (XRF) method.

Table 1: Chemical compositions of alloys (wt.%)

Alloy	Nominal alloys	Al	Zn	Mn	Si	Ca	Sm	Mg
A1	AZ91	8.97	0.70	0.21	-	-	-	Bal.
A2	AZ91-1.5Sm	8.77	0.69	0.22	-	-	1.43	Bal.
A3	AZ91-1.5Sm-0.8Si	8.89	0.66	0.21	0.77	-	1.48	Bal.
A4	AZ91-1.5Sm-0.8Ca	8.90	0.77	0.22	-	0.79	1.45	Bal.

The alloys were prepared in an electric resistance furnace under the protective atmosphere of CO_2 and SF6. Mg-30Sm, Mg-10Si and Mg-20Ca master alloys were added to the melt at 730 °C. The melt was manually stirred for about 3 min, and then, at 730 °C, was poured into a steel mould (preheated at 200 °C) having a 50 mm diameter and an 80 mm height. Some specimens were homogenized at 410 °C for 20 h and then quenched in 20 °C water (T4 treatment). Subsequent aging treatment was carried out at 200 °C for 4 h (T6 treatment). Metallographic samples were etched in acetic-picric acid (2.1 g picric acid, 5 ml acetic acid, 5 ml H_2O and 35 ml ethanol) for 10 s. The microstructure was characterized by an optical microscope and a scanning electron microscope (SEM) equipped with a energy-dispersive X-ray spectroscope (EDS). Phase identification was conducted by an X-ray diffraction (XRD) using Cu Kα radiation. The average grain size was measured by the linear intercept method. Differential scanning calorimetry (DSC) was conducted to analyze the phase transition under Ar atmosphere. The heating rate was 10 °C·min^{-1} and the scanned temperature interval was from room temperature to 650 °C. Tensile tests were conducted at room temperature at a strain rate of 2 mm·min^{-1}. The gauge length and diameters of tensile specimens were 28 mm and 5 mm. At least three specimens were used to obtain mechanical properties.

2 Results and discussion

2.1 Microstructure of as-cast alloys

The optical microstructures of the as-cast alloys are shown in Fig. 1. Figure 1(a) shows that the as-cast AZ91 alloy (alloy A1) mainly consists of dendritic α-Mg matrix and β-$Mg_{17}Al_{12}$ eutectic compounds distributing along the grain boundaries. Addition of Sm element in Fig. 1(b) (alloy A2) leads to the reduction of the β-$Mg_{17}Al_{12}$ phase. The additions of 0.8Si or 0.8Ca to AZ91-1.5Sm (alloys A3 and A4) in Figs. 1(c) and (d) further lead to the grain refinement. The coarse blocked-like Mg_2Si particles are observed at the grain boundaries in alloy A3.

Figure 2 shows the SEM micrographs and corresponding EDS results of the alloys A1, A2, A3 and A4. It can be found that the microstructures of the AZ91 alloy contain α-Mg matrix, (α-Mg + β-$Mg_{17}Al_{12}$), β- $Mg_{17}Al_{12}$ and Al_4Mn phases in Fig. 2 (a). When 1.5 wt.% Sm was added to AZ91, additional intermetallics of Al_2Sm and $Al_{11}Sm_3$ phases were observed in Fig. 2 (c), and the EDS analysis is shown in Figs. 2 (d) and (e). Furthermore, intermetallics of Al-Mn-Sm with atomic percentage ratio of 54.89:15.88:4.73 (the balance is Mg), are observed inside the grains according to SEM/EDS analysis.

With the additions of Si and Sm in Fig. 2 (f), new dark gray phases of block-shaped formed in addition to the intermetallic compounds of the Al-Sm. EDS analysis in Fig. 2 (g) showed that the block-shaped phase was Mg_2Si. In Fig. 2 (h), the addition of Ca to AZ91-Sm led to the formation of the fish-bone Al_2Ca intermetallics. Since Ca has nearly zero solubility in Mg and Al at room temperature [21], it segregated at the grain boundaries as Al_2Ca phase as shown by EDS analysis in Fig. 2 (i). Some intermetallics of Al-Sm-Ca formed in the matrix as shown in Fig. 2 (j), which was also observed by Chen Y A, et al [8]. Some intermetallics of Al-Mn, Al-Mn-Ca and MgAlCa were also found in Alloys A3 and A4.

Figure 3 shows the XRD patterns of the studied alloys. The diffraction peaks of AZ91 alloys in Fig. 3 (a) revealed several rising peaks of α-Mg and β-$Mg_{17}Al_{12}$ phases, which agreed

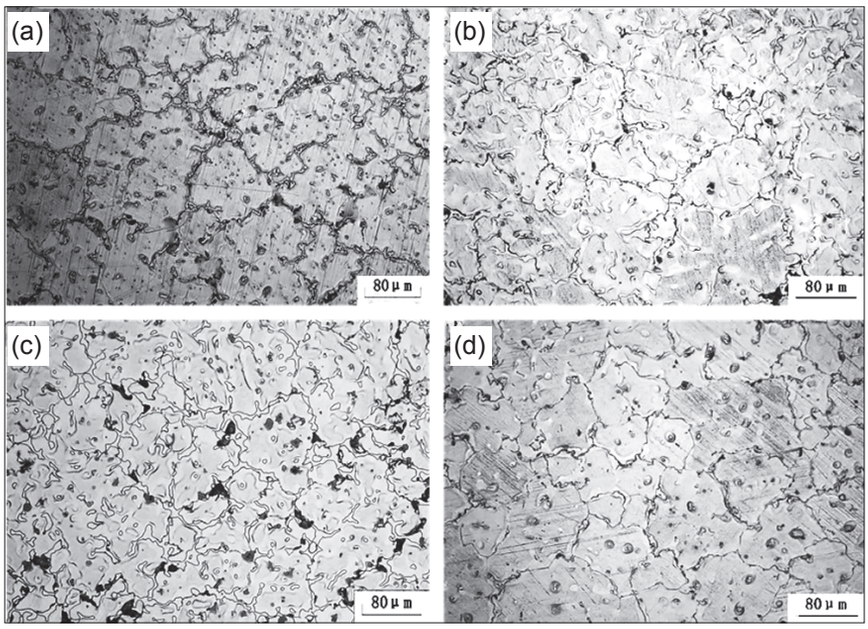

Fig. 1: Microstructures of as-cast alloys: (a) A1; (b) A2; (c) A3; (d) A4

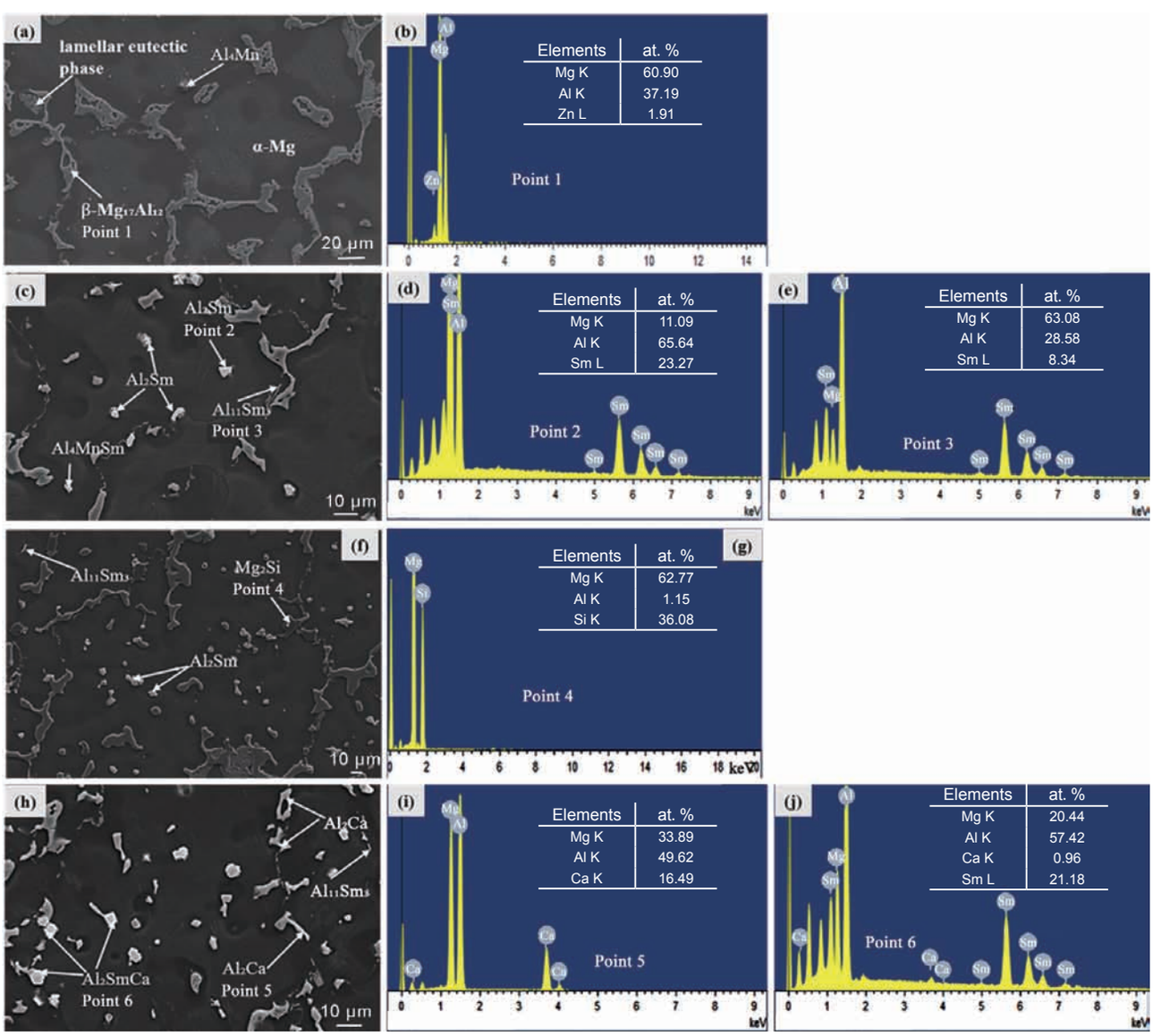

Fig. 2: SEM images of as-cast alloys: (a) A1; (c) A2; (f) A3; (h) A4; (b), (d), (e), (g), (i) and (j) EDS analysis of respective intermetallics formed

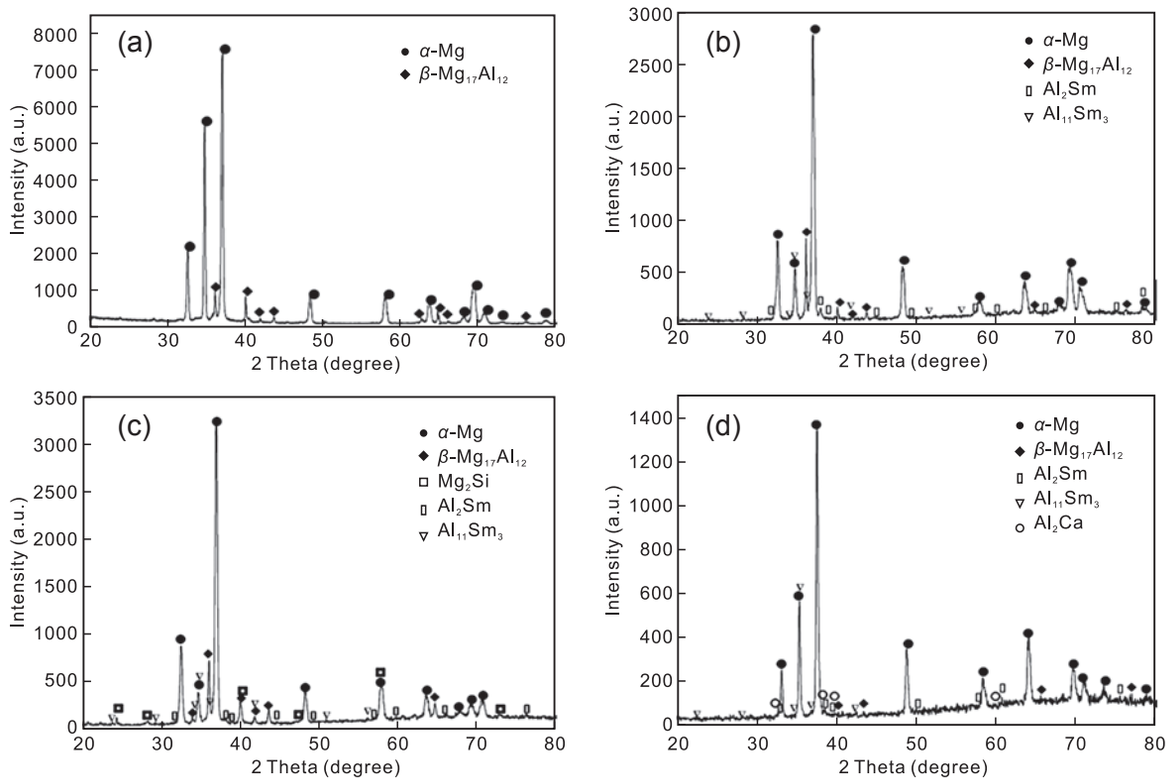

Fig. 3: XRD patterns of as-cast alloys: (a) A1; (b) A2; (c) A3; (d) A4

with the observation in SEM micrograph in Fig. 2 (a). The addition of Sm to AZ91 alloy resulted in extra peaks of Al_2Sm and $Al_{11}Sm_3$ as shown in Fig. 3 (b). Figures 3 (c) and (d) show that alloys AZ91-1.5Sm-0.8Si/Ca are consisted of the α-Mg, β-$Mg_{17}Al_{12}$, Al_2Sm, $Al_{11}Sm_3$, and Mg_2Si or Al_2Ca phases.

Figure 4 shows the DSC curves of the as-cast alloys. As shown in Fig. 4, the Curve 1 showed two endothermic peaks, suggesting the α-Mg matrix and eutectic phase. Sm and Si additions to the binary AZ91 alloy (Curves 2 and 3) did not affect the types of phase transformations of the based alloy. A small endothermic peak at 426.83–436.07 °C related to the transformation of β-$Mg_{17}Al_{12}$ phase is detected in Curves 1 to 3. Their corresponding peaks which represent the melting

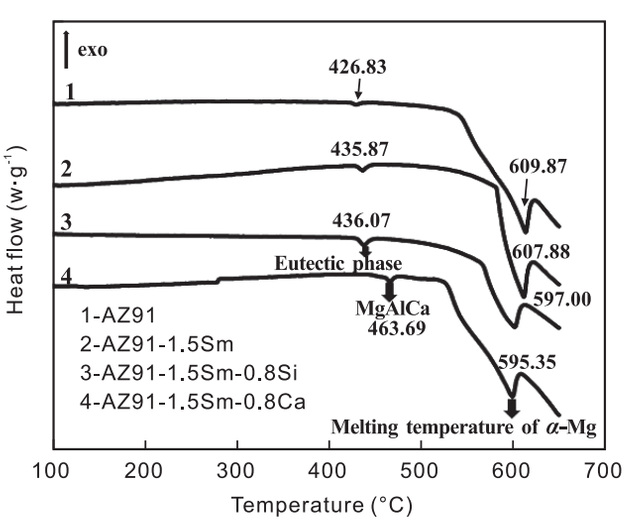

Fig. 4: DSC solidification curves of as-cast alloys

temperature of the α-Mg matrix are at 597.00–609.87 °C. In AZ91-Sm-Ca, the peak of the primary eutectic phase on the Curve 4 has a higher melting temperature of 463.69 °C, which can be considered as the decomposition temperature of the MgAlCa phase; the corresponding melting temperature of the α-Mg matrix is at 595.35 °C.

2.2 Microstructures of solid solution alloys

Figure 5 shows the solution treated microstructures of various alloys at 410 °C for 20 h. Figure 6 shows the calculated average grain size. It can be seen in Fig. 5 (a) that the β-$Mg_{17}Al_{12}$ phase has dissolved in the solutionized AZ91 alloy. Figures 5 (b–d) show the solutionized AZ91-1.5Sm, AZ91-1.5 Sm with 0.8 Si or Ca alloys, respectively. In AZ91-1.5Sm, the microstructure and grains of the solutionized alloy shown in Fig. 5 (b) is remarkably refined and the high-melting point Al_2Sm phase is spotted in the center of the grains, indicating some possible heterogeneous nuclei for the Mg grains. In addition, the segregation of some Sm atoms in the form of $Al_{11}Sm_3$ intermetallic contributes to the grain refinement mechanism. Also, Al_4MnSm particles are found in the center of the grains. Thus, it may be said that the Al_4MnSm and Al_2Sm compounds formed heterogeneous nucleation particles, and the segregation of $Al_{11}Sm_3$ at the grain boundaries is responsible for the effective refinement of the Mg grains. The alloy containing 1.5wt.% Sm shows a homogeneous microstructure with an average grain size of 91.98 ± 1.99 μm compared to the AZ91 alloy with an average grain size of 239 ± 16.94 μm.

With additions of Si and Sm to the AZ91 alloy in Fig. 5 (c), the high-melting point Al_2Sm phases are still marked and some Mg_2Si intermetallics segregate massively at the grain

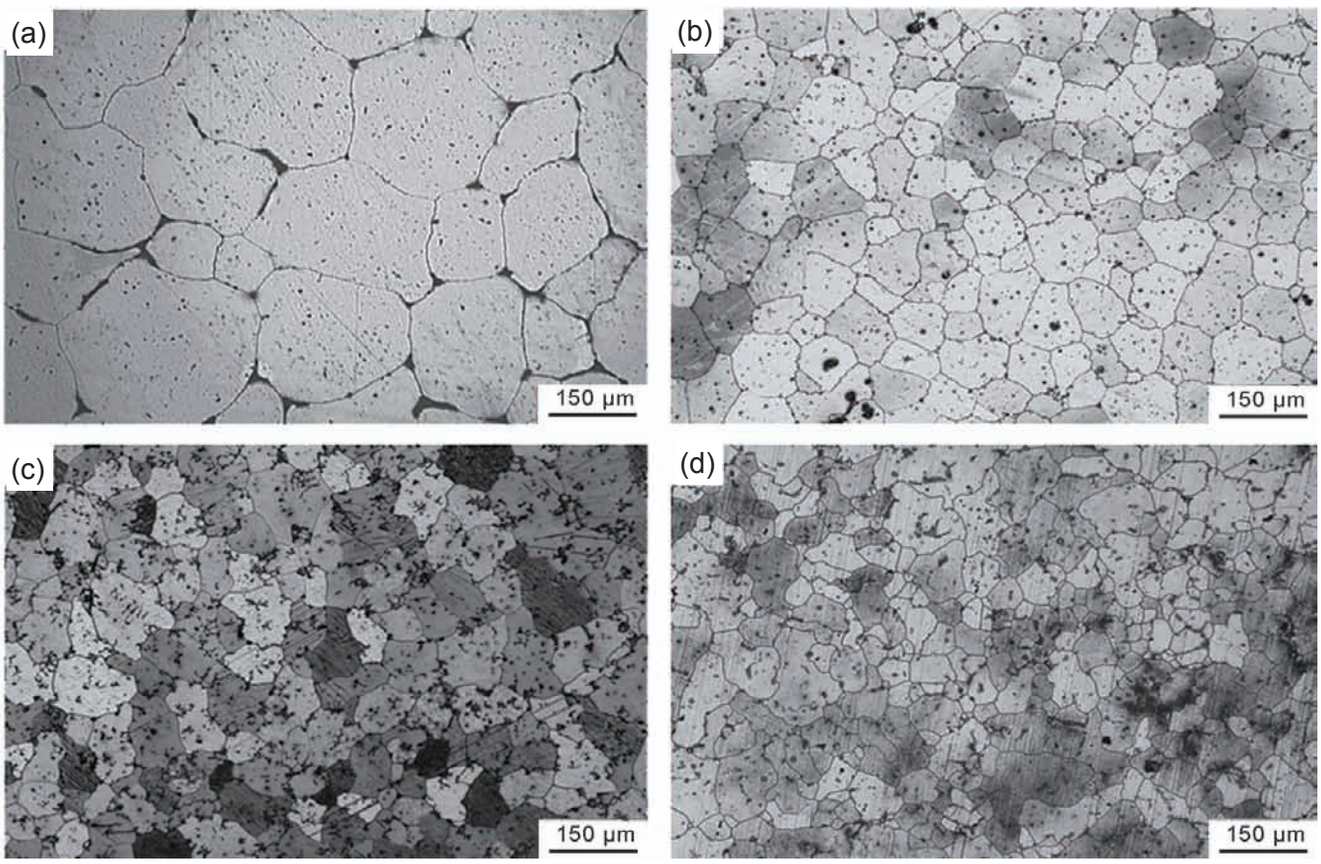

Fig. 5: Microstructures of alloys after solution treatment at 410 °C for 20 h and water-quenched: (a) A1; (b) A2; (c) A3; (d) A4

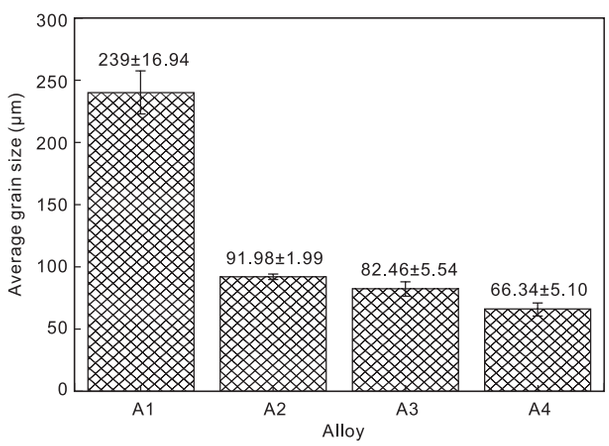

Fig. 6: Average grain sizes of varous alloys

boundaries. The average grain size further decreased to 82.46 ± 5.54 μm. Additions of Ca and Sm elements to the AZ91 alloy as shown in Fig. 5 (d) shows the significant grain size reduction with an average grain size of 66.34 ± 5.10 μm. In this alloy, some intermetallic particles believed to be the Al_2Sm intermetallic are still noted in the grain centers and some Al_2Ca particles concentrate at the grain boundaries. The calculated growth restricting factor (GRF) values for the individual solute elements, Si and Ca, are 9.25 and 11.94, respectively [3, 22], indicating that Si or Ca addition to Sm strongly segregates at the grain boundaries which can contribute to further grain refinement by restricting growth of the grains.

2.3 Microstructures of aged alloys

Figure 7 shows the optical microstructures of the aged alloys at 200 °C for 4 h after solutionizing and water-quenching. The dark gray regions at the grain boundaries and inside the grains shown in Fig. 7 (a) are indications of the presence of discontinuous precipitates of the β-$Mg_{17}Al_{12}$ phase in AZ91 alloy. Figures 7 (b–d) show that the quantity of discontinuous precipitates decrease in the aged AZ91-Sm, AZ91-Sm-Si and AZ91-Sm-Ca alloys and some intermetallics of Al_2Sm, Mg_2Si and Al_2Ca are found. The reasons for the decrease in discontinuous precipitates are the presence of heterogeneous nuclei which causes crystal defects within the matrix [23], and the growth restriction effect which lowers the nucleation rate and growth of discontinuous precipitates.

2.4 Tensile properties

Results of room temperature mechanical properties testing of as-cast samples are shown in Fig. 8 (a). The yield strength (YS) and ultimate tensile strength (UTS) of the as-cast AZ91 alloys with minor additions of Sm, and Si or Ca are higher than AZ91 alloy, indicating improvements in mechanical properties of the alloys. AZ91-Sm-Ca alloy has the optimum YS and UTS of 135 MPa and 199 MPa, respectively, which can be ascribed to grain refinement strengthening. On the other side, the Al_2Ca particles formed are brittle and coarse, which could subsequently worsen the EL of the alloy at

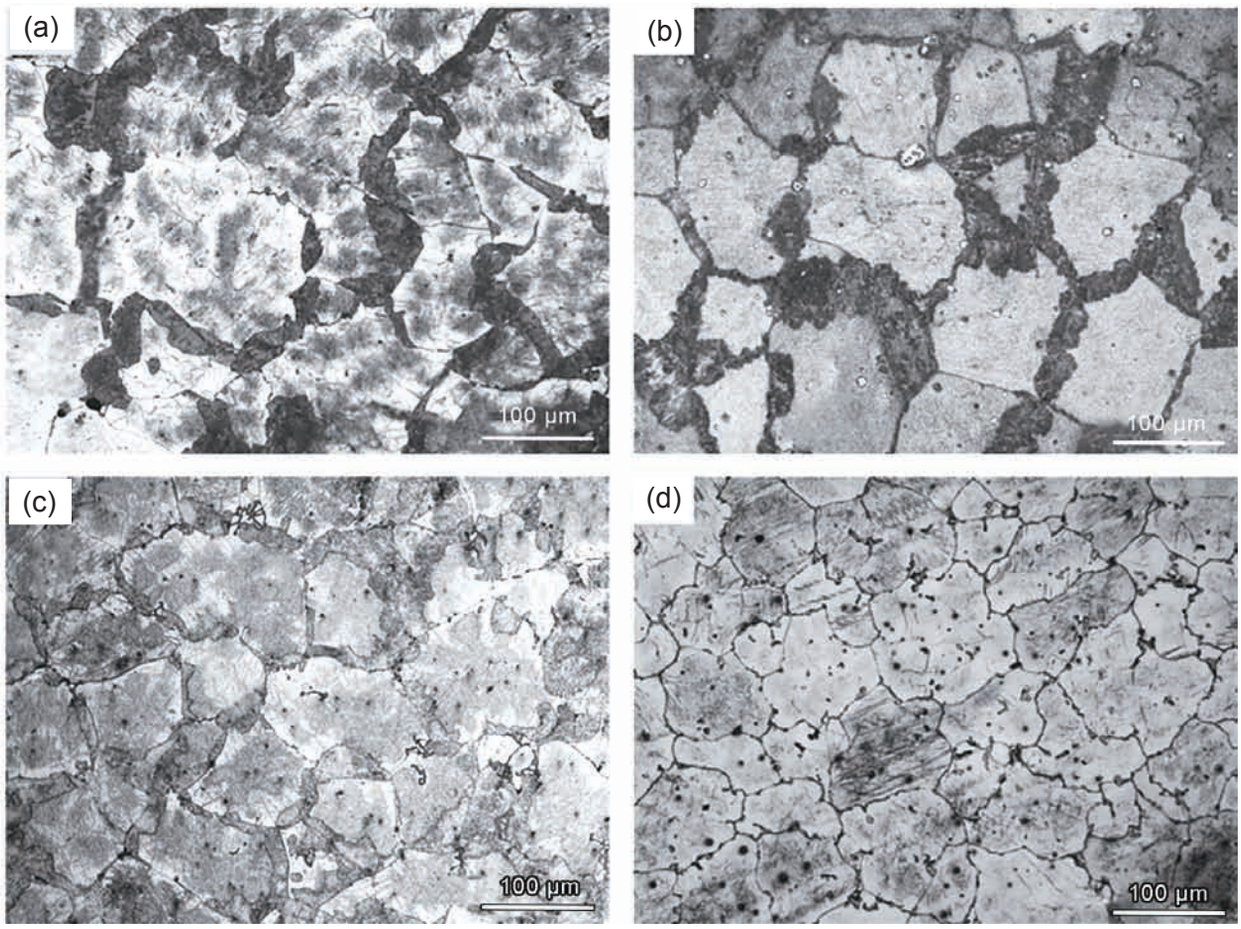

Fig. 7: Optical micrographs of alloys after T6 treatment at 200 °C for 4 h: (a) A1; (b) A2; (c) A3; (d) A4

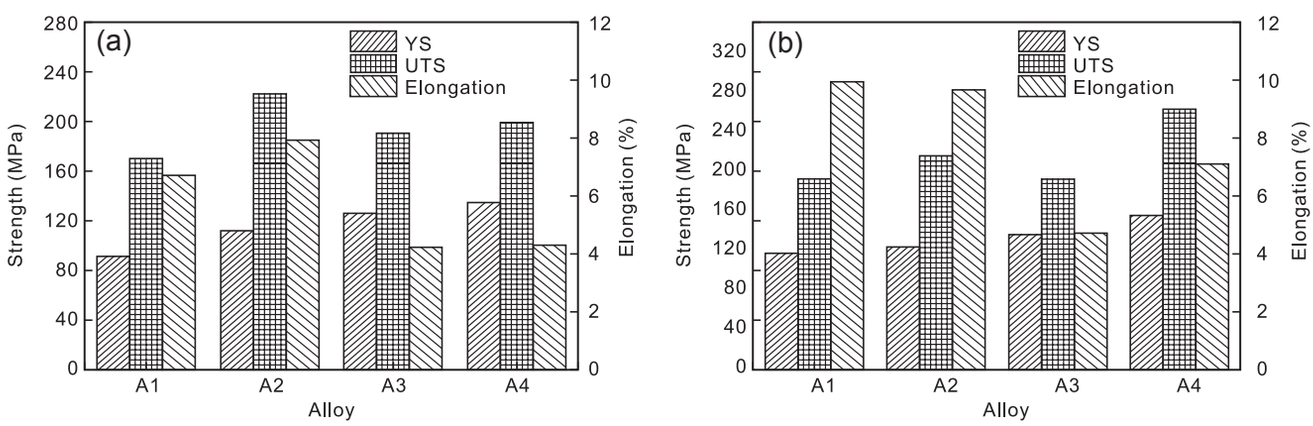

Fig. 8: Tensile properties of as-cast (a) and T6 alloys at room temperature (b)

room temperature. The mechanical performances of the alloys in terms of YS, UTS and EL with or without element additions increase after T6 treatment, as shown in Fig. 8 (b). However, the observable Mg_2Si phase in Fig. 7 (c) after aging contributes to the comparatively low UTS and EL in alloy A3. The improvements in yield and ultimate tensile strengths in the AZ91-Sm-Ca alloy can be attributed to grain refinement strengthening and reduction in discontinuous precipitates.

3 Conclusions

(1) The as-cast microstructure of AZ91-1.5 Sm alloy consists of intermetallic compounds of Al-Sm (Al_2Sm and $Al_{11}Sm_3$) and Al-Mn-Sm, α-Mg and β-$Mg_{17}Al_{12}$ phase. Moreover, adding minor Sm additions to AZ91 alloy could refine the grains of the alloy and a substantial grain refinement of 91.98 ± 1.99 μm was recorded.

(2) In AZ91-1.5Sm-0.8Si/Ca alloys, the morphologies of

β-$Mg_{17}Al_{12}$ particles were modified and refined and their growth patterns became discontinuous, and the average grain sizes were 82.46 ± 5.54 μm and 66.34 ± 5.10 μm, respectively.

(3) The as-cast YS and EL of AZ91-Sm-Ca are 135 MPa and 4.32%, respectively. The improvements in the YS were due to grain refinement strengthening. The alloy possessed YS of 154 MPa with EL of 7.1% at T6 treatment, which was ascribed to grain refinement strengthening and reduction in discontinuous precipitates.

References

[1] Mordike B L, Ebert T. Magnesium: Properties-applications-potential. Materials Science & Engineering A, 2001, 302(1): 37–45.
[2] StJohn D H, Qian M, Easton M A, et al. The interdependence theory: the relationship between grain formation and nucleant selection. Acta Materialia, 2011, 59(12): 4907–4921.
[3] StJohn D H, Qian M, Easton M A, et al. Grain refinement of magnesium alloys. Metallurgical and Materials Transactions A, 2005, 36(7): 1669–1679.
[4] Kumar P, Mondal A K, Chowdhury S G, et al. Influence of additions of Sb and/or Sr on microstructure and tensile creep behaviour of squeeze-cast AZ91D Mg alloy. Materials Science & Engineering A, 2017, 683: 37–45.
[5] Liu S F, Liu L Y, Kang L G. Refinement role of electromagnetic stirring and strontium in AZ91 magnesium alloy. Journal of Alloys and Compounds, 2008, 450: 546–550.
[6] Wang J L, Wang L D, Wu Y M, et al. Effects of samarium on microstructures and tensile properties of Mg-5Al-0.3Mn alloy. Materials Science & Engineering A, 2011, 528(12): 4115–4119.
[7] Sun M, Hu X Y, Peng L M, et al. Effects of Sm on the grain refinement, microstructures and mechanical properties of AZ31 magnesium alloy. Materials Science & Engineering A, 2015, 620: 89–96.
[8] Chen Y A, Jin L, Fang D, et al. Effects of calcium, samarium addition on microstructure and mechanical properties of AZ61 magnesium alloy. Journal of Rare Earths, 2015, 33(1): 86–92.
[9] Wang C L, Dai J C, Liu W C, et al. Effect of Al additions on grain refinement and mechanical properties of Mg-Sm alloys. Journal of Alloys and Compounds, 2015, 620: 172–179.
[10] Guan K, Li B S, Yang Q, et al. Effects of 1.5 wt% samarium (Sm) addition on microstructures and tensile properties of a Mg-6.0Zn-0.5Zr alloy. Journal of Alloys and Compounds, 2018, 735: 1737–1749.
[11] Hu Z, Liu R L, Kairy S K, et al. Effect of Sm additions on the microstructure and corrosion behavior of magnesium alloy AZ91. Corrosion Science, 2019, 149: 144–152.
[12] Hu Z, Li X, Hua Q, Yan H. Effects of Sm on microstructure and corrosion resistance of hot-extruded AZ61 magnesium alloys. Journal of Materials Research, 2015, 30: 3671–3681.
[13] Hu Y, Yu Nan, Zhao L Z, et al. Effect of Sm on the microstructure and properties of Mg-9Al alloy. International Journal of Cast Metals Research, 2017: 1–5.
[14] Li X, Hu Z, Yan H, et al. Effect of Sm-Rich phase on corrosion behavior of hot extruded AZ31-1.5Sm magnesium alloy. Journal of Materials Engineering and Performance, 2018: 1–11.
[15] Hu X Y, Fu P H, StJohn D, e al. On grain coarsening and refining of the Mg-3Al alloy by Sm. Journal of Alloys and Compounds, 2016, 663: 387–394.
[16] Zhang X M, Hu J L, Ye L Y, et al. Effects of Si addition on microstructure and mechanical properties of Mg-8Gd-4Y-Nd-Zr alloy. Materials & Design, 2013, 43: 74–79.
[17] Lü Y Z, Wang Q D, Zeng X Q, et al. Effects of silicon on microstructure, fluidity, mechanical properties, and fracture behaviour of Mg–6Al alloy. Materials Science and Technology, 2001, 17(2): 207–214.
[18] Lu Y Z, Wang Q D, Zeng X Q, et al. Effect of Si on the precipitation behavior of Mg-6Al alloy. Journal of Materials Science Letters, 2001, 20(5): 397–399.
[19] Li S S, Tang B, Zeng D B. Effects and mechanism of Ca on refinement of AZ91D alloy. Journal of Alloys and Compounds, 2007, 437(1-2): 317–321.
[20] Kawabata H, Yagi Y, Aoki Y, et al. Effect of Calcium on the combustion behavior of molten AZ91 magnesium alloy. Materials Transactions, 2018, 59(2): 272–279.
[21] Yue C F, Huang S J, Chen J K, et al. Effects of neodymium and calcium on the thermal stability of AZ71 magnesium alloys. Metals and Materials International, 2018, 24(2): 307–313.
[22] Easton M A, Qian M, Prasad A, et al. Recent advances in grain refinement of light metals and alloys. Current Opinion in Solid State and Materials Science, 2016, 20(1): 13–24.
[23] Braszczyńska-Malik K N. Discontinuous and continuous precipitation in magnesium–aluminium type alloys. Journal of Alloys and Compounds, 2009, 477(1–2): 870–876.

This work was financially supported by the National Key Research and Development Program of China (2016YFB0701204).